Green Chemistry

PAPER

View Article Online
View Journal | View Issue

Cite this: *Green Chem.*, 2020, **22**, 2786

Humin based resin for wood modification and property improvement†

Anna Sangregorio,[a,b] Anitha Muralidhara,[a,c] Nathanael Guigo, *[b] Lisbeth G. Thygesen,[d] Guy Marlair,[c] Carlo Angelici,[a] Ed de Jong[a] and Nicolas Sbirrazzuoli[b]

This study presents a novel process of wood modification employing humins, *i.e.* polydisperse furanic macromolecules formed during sugar dehydration. Humin valorization is more and more in the spotlight, thanks to the increased research efforts being placed by industries on biomass valorization. Here, a water soluble liquid fraction of humins was employed to impregnate wood and was polymerized within the wood using heat. This so-called 'humination' process was compared with the more classical furfurylation, which consists of impregnating with furfuryl alcohol (FA), and the polymerization of FA inside the wood. Confocal laser scanning fluorescence microscopy proved that furanic entities contained in the liquid fraction of humins polymerized within the wood cell walls and resulted in fluorescence similar to that seen for furfurylated wood. The humin modified wood showed lower mass increase and identical dimensional stability compared to furfurylated wood after immersion in water. Both treatments resulted in higher hydrophobicity compared to untreated wood. The elastic modulus of humin treated wood, measured by dynamic mechanical analysis (DMA), was similar to that of furfurylated wood for $T < 75$ °C and slightly higher than untreated wood. Finally, reaction-to-fire properties were investigated. Humin treated wood showed some advantages over furfurylated wood such as longer ignition time, slower heat release rate (−13%) and lower CO formation. This study demonstrates for the first time that humins can be used as an alternative to FA for wood modification to obtain enhanced wood products.

Received 21st October 2019,
Accepted 13th January 2020

DOI: 10.1039/c9gc03620b

rsc.li/greenchem

Introduction

There is growing interest in developing materials from renewable resources instead of non-renewable ones. Valorization of lignocellulosic biomass is one of the most promising solutions to mitigate climate change and the depletion of fossil feedstocks worldwide.[1,2] Wood is one example of lignocellulosic biomass resources and has been used for millennia.[3,4] Its particular physical and mechanical properties combined with low density and high long-term carbon storage potential make wood a good candidate for building applications. For these types of applications, wood often needs to be in contact with the environment.[3,5,6] To guarantee long-life wood products good dimensional stability and resistance towards fungal and bacterial degradation are required, which is lacking in most softwoods. Traditionally the latter has been solved by impregnation with biocides, while wood modification offers a more environmentally benign solution to both problems by reducing the moisture content of the material to levels that ensure dimensional stability and prevent biological degradation.[7] Thus, moisture exclusion through wood modification provides protection against fungal degradation without adding biocidic properties to the material.[8] Another problem of unmodified softwood is its combustible nature, which may also play a critical role in leading to altered fire risks.

One of the most environmentally friendly chemical modifications of wood is *furfurylation*, which consists of the polymerization of furfuryl alcohol (FA) within the wood cell wall. FA is a biobased platform molecule easily obtained *via* hydrogenation of furfural, usually derived from agricultural residues such as rice hulls, bagasse, and corncobs. FA polymerization to poly(furfuryl alcohol) (PFA) is catalyzed by acids, leading to a strong reticulated network.[9,10] The final furfurylated wood has thermomechanical properties similar to tropical wood and does not show any toxicity problems exceeding those of natural heartwood.[11,12] Furfurylated wood is a growing com-

[a]*Avantium Chemicals B.V., Zekeringstraat 29, 1014 BV Amsterdam, The Netherlands*
[b]*Université Côte d'Azur, Institut de Chimie de Nice, CNRS, UMR 7272, 06108 Nice, France. E-mail: Nathanael.Guigo@univ-cotedazur.fr*
[c]*Institut national de l'environnement industriel et des risques (INERIS), Parc technologique Alata, BP 2, Verneuil-en-Halatte, Picardie, France*
[d]*University of Copenhagen, Department of Geosciences and Natural Resource Management, Rolighedsvej 23, 1958 Frederiksberg C, Denmark*
†Electronic supplementary information (ESI) available. See DOI: 10.1039/c9gc03620b

mercial product marketed by the company Kebony (Skien, Norway) under the company's name.[13]

Humins are another example of biomass derived material, and are co-products of the acid-catalyzed conversion of carbohydrates, cellulose, and hemicellulose into platform chemicals. Humins are heterogeneous and polydisperse macromolecules mainly constituted of furanic rings with aldehydes, ketones and hydroxyls as main functional groups.[14–17] Humins have many similarities with PFA, and thus could be used as a possible alternative to furfuryl alcohol in the modification of wood, provided that they are able to enter the wood cell walls even though they are oligomers in contrast to the monomeric FA. Moreover, thanks to the growing industrial interest in green chemistry and biomass conversion, humin valorization is becoming more and more important.[1,2,14,18–21]

This study focuses on the preparation of modified wood with a water soluble fraction of humins from a biorefinery process. First this liquid fraction of humins was properly characterized in terms of chemical structure and physico-chemical properties. Then, humin-modified wood was compared with PFA modified wood and untreated wood. Wood was first impregnated under vacuum to promote penetration into the wood cell of either the liquid fraction of humins or a FA/water solution. After cross-linking, the distribution of the humins or PFA within the wood tissue was studied using confocal laser scanning fluorescence microscopy (CLSM) and FTIR measurements allowed the investigation of interaction with wood components. The performance of the modified wood with regard to its dimensional stability, mechanical properties and fire properties was also explored.

Materials and methods

Materials

Humins were supplied by Avantium N.V. and produced in their pilot plant in Geleen, the Netherlands, by the dehydration of fructose and glucose. Furfuryl alcohol (FA) (purity: ≥98%) as the monomer and maleic anhydride (MA) (purity: ≥99%) as the catalyst were purchased from Sigma-Aldrich and used as received. Untreated pinewood veneers were purchased from Amsterdamsche Fijnhouthandel, Amsterdam, The Netherlands.

Resin preparation and wood impregnation

Humins were heated in an oil bath and mixed at 80 °C for 20 minutes. Demineralized water, preheated at 80 °C, was added to humins by stirring in a humins/H_2O ratio of 50/50% in weight. After 40 minutes the mixture was taken out of the oil bath and allowed to cool down. Once at room temperature, the mixture separates into two phases: a solid residue and a liquid phase respectively composed of 65 wt% and 35 wt% of the initial humins. The decantation in two phases (the solid and liquid phase) proceeded for 2 hours at room temperature. This so-called *liquid fraction of humins*, consisting of around 55 wt% of H_2O and 45 wt% of the humin phase, was recovered and was employed to impregnate wood without any extra acidic catalyst. For wood impregnation the liquid fraction of humins was employed (with a humins/water ratio of 45/55 wt%). On the other hand, the physico-chemical characterization of the liquid fraction of humins was done on dried samples *i.e.* after complete water removal at 60 °C.

Another FA based mixture was prepared to compare with the liquid fraction of humins. FA was mixed with 2 wt% of MA for 15 min at 80 °C. Demineralized water was added to the mixture in a FA/MA/H_2O ratio of 49/1/50 wt% in order to have a similar amount of water compared to the liquid fraction of humins as well as an expected weight percent gain (WPG) of around 30%, *i.e.* the lowest value known from the literature to extend the expected durability of wood samples in ground and marine contact compared to untreated wood[12,22] and therefore suggested as the WPG to use commercially.[23] Moreover the anti-swelling efficiency levels off at 30% of WPG. This means that no more FA can be polymerized into the cell wall for WPG > 30%.[7] The FA mixture was stirred for 5 minutes at 80 °C to obtain a homogeneous liquid phase.

Wood veneers (2 mm thick) were dried under vacuum at 60 °C for one hour before impregnation. The vacuum pressure was about 2 mbar. Before vacuum impregnation, the veneers were completely covered either with the liquid fraction of humins or the FA mixture. In each case, the quantity of impregnating solution was set to obtain, after complete treatment, a weight percent gain (WPG) of about 30 wt% compared to the untreated wood. Samples with a lower WPG were attempted (*i.e.* with a lower quantity of impregnating solution) but resulted in non-homogeneous samples. The samples were placed under vacuum at 60 °C (vacuum pressure ~2 millibar) for one hour to promote impregnation. The samples were then taken out of the solution, the surface was gently dried with a cloth and the samples were cured in an oven for 1 hour at 150 °C. The impregnated samples were compared with wood veneers which had been subjected to the same treatments as the impregnated samples, *i.e.* dried in a vacuum oven for one hour at 60 °C, impregnated with pure water and then heated for one more hour at 150 °C. For humin treated wood and PFA treated wood, the final WPG was 30 ± 2%.

Size exclusion chromatography (SEC)

The SEC apparatus was a Bio-inert Agilent 1260 HPLC system for the analysis of liquid samples, equipped with a diode-array detector (DAD), refractive index detector (RI) and sample collector. The column was an Agilent PLgel 3 μm Mixed-E 10 × 300 mm plus an Agilent PLgel 3 μm Guard. The column temperature was set to 40 °C. The injection volume was 50 μL and the mobile phase was tetrahydrofuran (analytical grade). Data acquisition was done with Agilent OpenLab. Data files were converted to Agilent GPC/SEC software in order to process the data and calculate the molar mass. Polystyrene standards were used to calibrate the system with 12 references in the range of M_w 266–M_w 62 500 g mol^{-1}. The humin samples (~15 mg) were diluted to approximately 2.5 mg ml^{-1} in THF. The samples were stirred for at least 1 min until complete dissolution, were left overnight and were centrifuged for 5 min at 12 500 rpm before injection.

^{1}H NMR spectroscopy

The NMR spectra of humin samples were recorded in deuterated acetone on a Bruker AVANCE III HD spectrometer operating at 400.17 MHz for ^{1}H. Experiments were recorded with a flip angle of 30°, and using sequences provided by Bruker. The spectrometer was equipped with the following probe: PA BBO 400S1 BBF-H-D-05 Z. The peak integrations were done with the Mestre Nova software.

Differential scanning calorimetry

Conventional DSC measurements were performed with a Mettler-Toledo DSC-1 heat-flux instrument, and STAR software was used for data analysis. Temperature, enthalpy, and tau lag calibrations were performed with indium and zinc standards. Crude humins and the liquid fraction of humins from the separation procedure described above (5–10 mg) were placed in a 40 μL aluminum crucible and closed with a pan lid, after drying 60 hours at 60 °C. Two consecutive runs were measured, with a scanning temperature ranging from −60 °C to 170 °C. Cooling/heating rates of 30 °C min^{-1} were employed.

Dynamic rheometry

Rheological properties were measured with a Thermo Scientific HAAKE MARS rheometer. Measurements were performed in plate–plate geometry (25 mm diameter and 1 mm gap). The linear viscoelastic region of samples was defined by a strain sweep. Viscosity was measured at 1 Hz at a strain below the critical strain at 40 °C.

Infrared spectroscopy

A Bruker tensor 27 – FTIR spectrometer equipped with a nitrogen-cooled MCT detector, was used to characterize samples using a 1 reflection diamond ATR device. The spectra of blank wood and modified wood were recorded. The spectrum of air was recorded as background before each measurement (64 scans). A total of 64 scans with a resolution of 2 cm^{-1} were recorded for each sample in the range from 4000 to 600 cm^{-1}, and are presented as absorbance spectra. Three spectra were recorded per sample. The spectra were normalized to 1 with the highest band at 1020 cm^{-1}. Prior to the FTIR measurement the different wood samples were completely dried under vacuum at 60 °C and were left to equilibrate in the atmosphere of the analytical room (~50% humidity). The FTIR measurements were performed after one week of equilibration.

Confocal laser scanning fluorescence microscopy (CLSM)

CLSM imaging was carried out using a Leica SP5-x microscope equipped with a white light laser. Wood specimens (untreated, humin treated and furfurylated) were water saturated in demineralized water, and 20 μm cross sections were cut using a Leica rotary microtome (Leica RM2255). The sections were mounted on glass slides in water under glass coverslips sealed with nail polish. Three different locations per sample type were investigated. For each location a fluorescence emission image in the range of 500–600 nm was taken for excitation at 488 nm, and one in the range of 640–690 nm for excitation at 633 nm. In addition, for each location pseudo-emission curves based on 10 nm steps after the same two excitations were recorded in the range 500–700 nm and 650–750 nm, respectively.

Scanning electron microscopy (SEM)

Blank wood and humins and PFA modified wood were investigated *via* scanning electron microscopy (SEM) at the microscopy center of the University of Nice Sophia Antipolis using a JEOL 6700F microscope equipped with a field emission gun. The electron beam voltage was fixed at 1 kV.

Dynamic mechanical analysis (DMA)

The dynamic mechanical properties were studied by dynamic mechanical analysis (DMA), Mettler-Toledo DMA-1 in tensile mode. Samples were tested on temperature sweeps from −40 °C to 180 °C with a heating rate of 2 °C min^{-1}. Experiments were done in a single frequency oscillation mode with a frequency of 1 Hz, force amplitude of 0.1 N and displacement of 0.05% in auto tension offset control. A preload of 0.5 N was applied.

Thermogravimetric analysis (TGA)

Thermogravimetric measurements were carried out on a TGA 851e from Mettler-Toledo. Samples were analyzed using a heating rate of 10 °C min^{-1} under air flow (50 mL min^{-1}). The samples were heated from 30 °C to 1000 °C.

Dimensional stability

The dimensional stability of untreated wood and modified wood was studied. The different wood samples were equilibrated at ~50% humidity during one week to reach their equilibrium moisture content. The mass and thickness of the samples were checked before immersion in water. The samples were then submerged for the desired period of time in water. The mass and thickness were checked every time the samples were taken out of the water, and the water was then replaced. The thickness was measured in three points and an average was considered. The samples were submerged in water for periods up to 120 hours.

The thickness increase was calculated by measuring the thickness of the samples before and after immersion in water, according to the following equation:

$$\text{Thickness increase}\,\% = \frac{t_f - t_i}{t_i} \times 100 \quad (1)$$

where t_f is the thickness after immersion in water and t_i is the thickness before immersion.

Mass increase was calculated by measuring the mass of the samples before and after immersion in water, using the following equation:

$$\text{Mass increase}\,\% = \frac{W_f - W_i}{W_i} \times 100 \quad (2)$$

where W_f is the mass after immersion in water and W_i is the mass before immersion.

Fire calorimetry

Fire calorimetry is the modern way to scientifically explore and assess the fire behavior of materials and products from the lab-scale to large scale.

For our study, we have selected the Fire Propagation Apparatus (FPA),[24–26] following the description and procedure of ISO 12136.[27] In the current study, combustion tests of composite samples of 10 × 10 cm were carried out under well-ventilated conditions, under 35 kW m^{-2} of external heat flux. Ignition was ensured by the use of a pilot flame. Full technical details of FPA operation are provided in the ESI.†

Results and discussion

Techno-economic and green chemistry considerations

Techno-economic considerations are quite important to highlight scientific breakthroughs that can have a practical industrial future. Recent reviews have highlighted the environmental benefits of modified wood (*i.e.* by acetylation or furfurylation) as alternative materials to tropical hardwoods.[28] Upon moderate weight percent gain (~30%) furfurylated wood presents significantly improved stiffness stabilization efficiency and anti-swelling efficiency (more than 50%) as well as good protection against biodegradation (fungi, marine borers and termites).[12] Such exceptional wood products have therefore led to commercial products with a strongly growing market share.[13] However, a factor hampering the growth of wood furfurylation is the fluctuating price of FA. Indeed, the cost of FA rose abruptly up to 3€ per kg in the last few years due to both supply and demand reasons.[29] Currently, the foundry resin segment is dominating the global FA market and is foreseen to account for more than 88% of the volume share in 2028.[30] Therefore, cost effective alternatives to FA in wood durification applications are very relevant to accommodate the foreseen growth in this application field. In that respect, humins offer several advantages from an economical point of view. Humins, as side-stream products obtained in a number of processes involving the upgrading and valorization of sugars do not yet have an established market price. The value that humins carry fully depends on the application, the urgency to replace a component (*e.g.* due to toxic considerations), the amount of humins required and the impact on the functionality of the end application. If the humins add functionality over the existing product, it is a good basis to achieve a higher price than for the product it replaces. If the same functionality is obtained but more material is required, a realistic price is likely to be below that of the product being replaced.[31] Humin commercialization can therefore help to stabilize the FA market. In the presented study only 35% of the raw humins are employed (*i.e.* the water soluble fraction) and for the remaining 65% other interesting applications, such as building blocks for thermoset resins or foams, have been identified.[18,32,33]

In the Twelve Principles of Green Chemistry introduced by Anastas and Warner,[34] principle four relates to the design of chemicals with reduced toxicity while the efficacy of the function is preserved. A recent paper shows that industrial humins from bio-refinery operations (the same as the humins employed here) do not present ecotoxicological concerns.[35] This is a key advantage for the eventual replacement of toxic chemicals. As a reactive monomeric chemical, FA is rather considered as an acute toxic substance (GHS06 label) as attested by the European Chemicals Agency[36] which can cause serious health damage (GHS08 label). FA may play a role in allergic airway disease which can cause problems in particular for work-related exposure.[37] China, the highest producer of FA in the world, has integrated the rules on FA toxicity leading to the reduction of production capacity, thereby contributing to the destabilization of the FA market.[29] Accordingly, replacing FA with humins might prevent these toxicological issues during manufacture and production. Nevertheless, the situation around the final product is very clear. Furfurylated wood is safe and does not show any additional ecotoxicity compared to untreated wood.[22]

The Green Chemistry principle number five is also met in the present investigation since the 'humination' of wood avoids the utilization of auxiliary substances – such as maleic anhydride – necessary to initiate and boost FA polymerization. Only the liquid fraction of humins is employed without the addition of extra chemicals.

Moreover, the environmental impacts linked to the modification processes (*i.e.* curing, drying *etc*.) should be taken into account. A recent investigation has shown that the life of furfurylated wood should be at least about two times the life of untreated wood to compensate for the modification process and to reach carbon neutrality.[38] As discussed earlier, the service life of furfurylated wood of moderate WPG (*i.e.* ~30% as in the present paper) is increased by at least 5 to 15 times depending on the conditions (marine or on shore environments).[12] This is much more than the required two times for reaching carbon neutrality thus outlining that furfurylation is clearly environmentally relevant. In addition, the very low maintenance of furfurylated wood (*i.e.* no coating, painting, varnish, *etc*.) compared to untreated wood also highlights the long-term positive impact of furfurylation on the environment.

To summarize, similar or increased properties of humin treated wood would make "humination" a very good strategy for wood treatments with some additional green advantages over furfurylation: more stable sourcing price, lower toxicity of humins compared to FA, no auxiliary chemicals needed and long-term valorization of industrial bio-production.

Chemical and physical characterization of the liquid fraction of humins used for impregnation

A liquid fraction of humins (*i.e.* water soluble fraction of humins) was employed to impregnate wood veneers instead of using raw industrial humins which are expected to contain more heterogeneous macromolecules with higher polydispersity and higher viscosity. Table 1 compares physico-chemical data obtained on raw humins and the liquid fraction of humins. These data have been obtained after having dried the

Table 1 Chemical and physical properties of raw humins compared to humins' fraction in the liquid phase. Humin assignment of major IR peaks of blank wood and humin resin

	M_w/g mol^{-1}	PD	^{1}H NMR integration ratio (furanic/aldehyde protons)	T_g/°C	Viscosity at 40 °C Pa^{-1} s^{-1}
Raw humins	4650	18	4.7	+2	3.1×10^3
Liquid fraction of humins	325	2.2	2.6	−6	1.2×10^2

samples to remove the water. First, the SEC data show that the molar mass and the polydispersity of the liquid fraction of humins are much lower compared to raw humins. This indicates that the fraction of humins that is water soluble is much less condensed than the raw humins since there is a difference of an order of magnitude. This would indicate that only lower molecular mass compounds are present in the liquid fraction with oligomers of a few furanic entities (around three/four furanic units). The molecular structures of the two humins' samples show similarities and differences. The ^{1}H-NMR spectra are presented in the ESI (Fig. SI-1†). The signal attributed to the aldehyde protons appears at δ = 9.55–9.58 ppm depending on the environment (in the vicinity of a furan ring or an alkyl group). The C3–C4 furanic protons present two doublets at δ = 7.35 ppm and 6.55 ppm. Finally, broad aliphatic peaks corresponding to methylenic protons close to hydroxyls or carbonyls present resonances between 2 ppm and 4.6 ppm. The integration can give information on the chain length. The ratio between the integration of aldehydes' protons on furanic protons (*i.e.* $I_{aldehydes}/I_{furanics}$) is presented in Table 1. This clearly demonstrates that the liquid fraction of humins contains more aldehyde end groups compared to raw humins. This indicates a lower amount of furan rings compared to raw humins thus resulting in shorter/less condensed chains, in agreement with the SEC data. In other words, it can be emphasized that the liquid fraction of humins contains more reactive aldehyde groups per furanic unit to connect with hydroxyls compared to raw humins. Finally the glass transition temperature (T_g) measured by DSC is lower for the humins' liquid fraction compared to raw humins (Table 1) as a consequence of the higher chain mobility due to the lower molar mass. Finally the dynamic viscosity measured at 40 °C is one order of magnitude lower for the humins' liquid fraction confirming shorter chain lengths or less condensed structures in this fraction compared to the initial materials.

According to these data, the liquid fraction of humins is more suitable for wood impregnation than the raw humins.

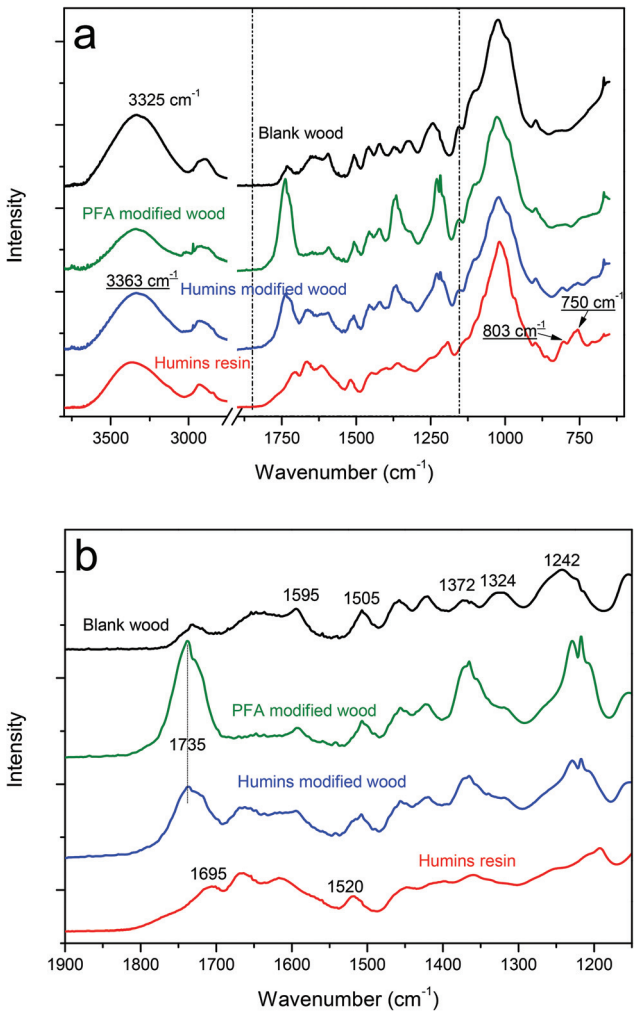

Fig. 1 (a) IR spectra of blank wood (black line), PFA modified wood (green line), humin modified wood (blue line) and humin resins (red line) (a) in the range 3800 cm^{-1}–700 cm^{-1} and (b) zoom on the region 1900 cm^{-1}–1100 cm^{-1}.

Interactions of humins or PFA with wood tissues

The IR spectra of untreated wood, PFA modified wood and humin-modified wood are shown in Fig. 1. For better interpretation, the FT-IR spectra of cured humin resin was also added. The latter was obtained by thermally treating the liquid fraction of humins in a vacuum and static oven, following the same process as for humin modified wood. This technique was used to investigate the possible interactions between humins resin and wood cell wall after the modification, albeit not all possible crosslinking to lignin is expected to be visible using this technique.[39] Fig. 1a shows the spectra of the three samples. Fig. 2B shows a zoom in the region 1900 cm^{-1}–1115 cm^{-1}. The assignment for the most significant peaks seen in blank wood and humin resin are reported in Table 2.[40–43]

A broad absorption band is observed in wood samples at 3000–3600 cm^{-1}, which indicates the presence of –OH stretching vibrations from wood cell wall biopolymers and from

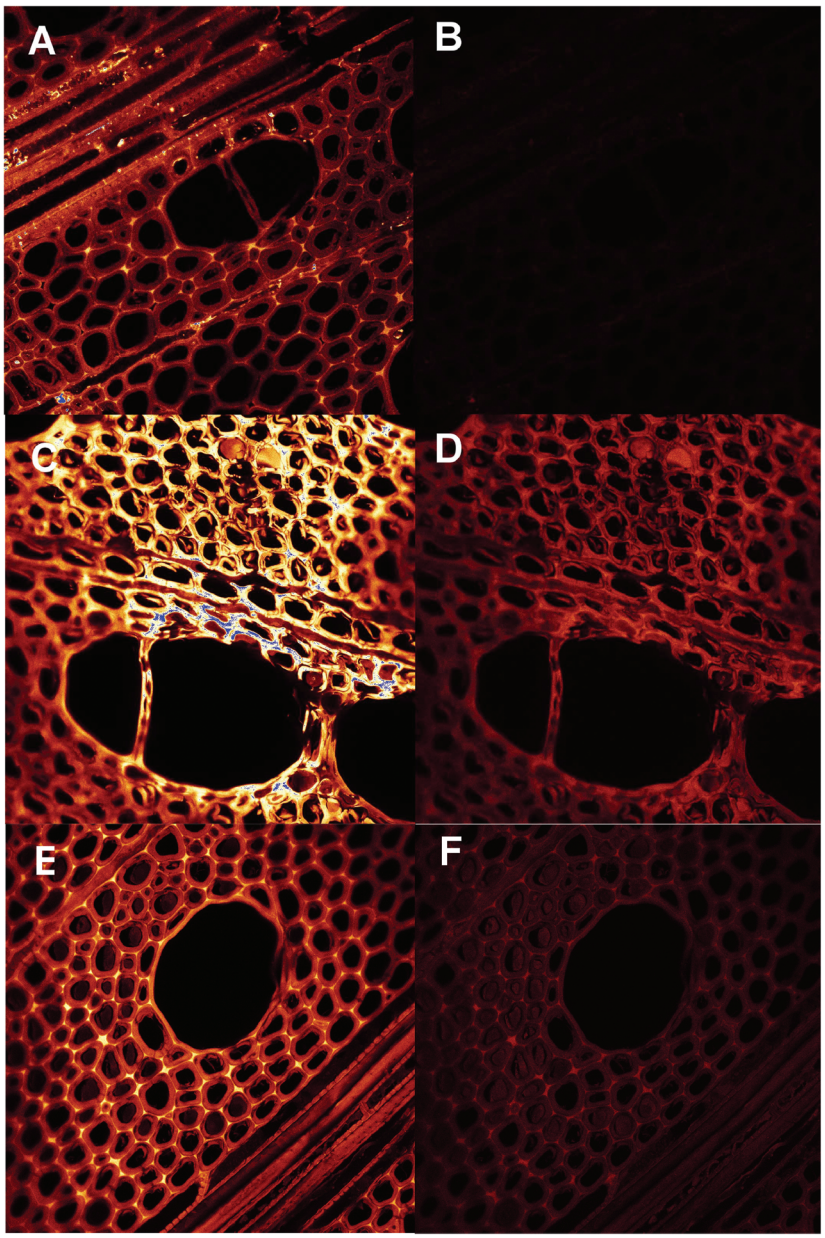

Fig. 2 CLSM emission images after excitation at 488 nm (first column) or 633 nm (last column) for untreated wood (A and B), furfurylated wood (C and D) and humin treated wood (E and F). Emission intensity is colour coded from black over brownish to yellow and white. Settings were standardized leading to different and thus comparable emission intensities of the images captured for different samples. Blue indicates detector overload. Each image shows an area of 246 × 246 μm. At least three different locations were studied per sample type with a similar outcome for the same treatment. Of these replicates one is shown here.

water. This band has lower intensity in modified wood (both PFA and humins) compared to untreated wood. A slight shift of the –OH peak position toward higher wavenumbers, from 3323 to 3346 cm^{-1}, is also observed after wood treatment. This shift to higher wavenumbers indicates changes in the H-bonded network. In particular, the bands of free –OH groups are located at higher wavenumbers than those of H-bonded –OH groups. This suggests that, after modification with humins and PFA, the environment of –OH groups of wood goes from more H-bonded to less H-bonded. The PFA and humin treatments contribute to increasing the hydrophobicity of wood, thus less water is absorbed from the environment (*i.e.* lower OH peak intensity compared to untreated wood) and less H-bonded functional groups are observed. The peak observed in untreated wood at 1735 cm^{-1} is associated with unconjugated C═O stretching in non-cellulosic structural polysaccharides such as hemi-cellulose. This peak is observed to significantly increase and slightly shift towards a higher wavenumber in humin and PFA modified wood, indicating the presence of new carbonyls. Indeed, humins and PFA contain

Table 2 Assignment of major IR peaks of blank wood from Lupoi *et al.*[45] and humin/PFA[1] resin

Blank wood assignment	Wavenumber (cm^{-1})
O–H stretching vibrations from cellulose	3325
Unconjugated C=O stretching of xylan	1735
Aromatic skeleton vibrations in lignin	1595, 1500, 1422
C–H deformation combined with aromatic ring vibration	1460
C–H deformation in cellulose and hemicellulose	1372
C–O stretching and C=O deformation in lignin and xylene	1243

Humin resin assignment	Wavenumber (cm^{-1})
O–H stretching	3363
C=O conjugated to alkene	1700
C=O conjugated to furan rings	1665
C=C in furan ring	1520
C–H out-of-plane deformation, furan ring	805
C–H wagging, furan ring	750

carbonyl groups, especially ketonic species from furan ring opening reactions. It has been shown that furan ring opening reactions occur preferentially when the polycondensation of FA occurs in water.[9] The same is observed for the peaks at 1372 and 1243 cm^{-1}. In untreated wood, these peaks correspond respectively to C–H deformation in holocellulose and C–O stretching and C=O deformation in lignin and xylene. In modified wood (both humins and PFA), the peaks at 1372 and 1243 cm^{-1} are more intense and shifted, again suggesting that furan ring opening reactions have occurred during furfurylation and humin cross-linking leading to additional C–H or C–O stretching. These ring opening reactions can occur in the presence of water during wood treatment thus leading to the increase in the signal of these open structures as already observed for the neat PFA resin.[9] In humin modified wood, the formation of hemiacetal functions as the result of cross-linking between aldehydes and hydroxyls from wood components might also occur. Indeed, the FTIR signature from hemiacetals appears between 1360 and 1400 cm^{-1} (ref. 44) and C–H deformation and aromatic skeletal vibration of lignin are observed in blank wood respectively at 1460 and 1595, 1500, 1422 cm^{-1}.[42] These peaks are not subjected to any variation after modification with humins. This might indicate that humins or PFA do not interact with the aromatic ring of lignin directly. As pointed out earlier likely bonding positions to lignin structures do not involve the aromatic rings, and would consequently not affect the 1500 and 1595 cm^{-1} bonds.[39] Modified wood shows new peaks at 1665 cm^{-1}, 1520 cm^{-1}, and in the region 805–750 cm^{-1}, associated with humin resin. These peaks correspond respectively to carbonyl groups conjugated to furan rings, C=C and C–H in furan rings.[43] This indicates the presence of crosslinked humins within the wood structure similar to the case of PFA in furfurylated wood.

CLSM imaging showed that humin modified specimens contained fluorescent substances both throughout the cell wall and to some extend also in cell lumina (Fig. 2 and 3).

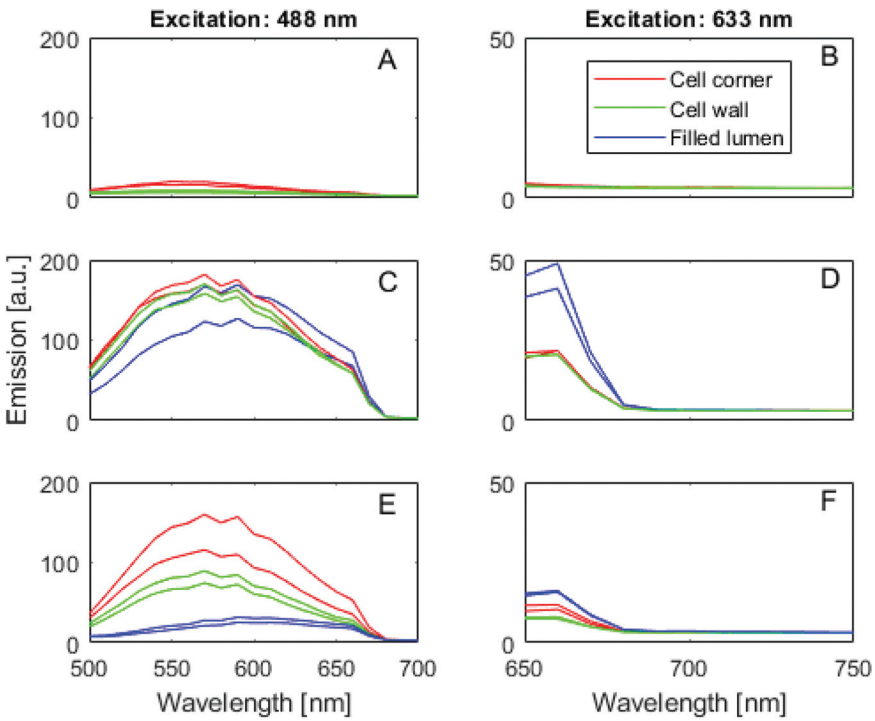

Fig. 3 CLSM-based pseudo-emission curves for untreated wood (A and B), furfurylated wood (C and D) and humin treated wood (E and F). Each curve corresponds to a particular region of interest selected from the images shown in Fig. 2, *i.e.* cell corners, S2 cell wall layer and polymer-filled lumina. At least three different locations were studied per sample type with a similar outcome for the same treatment. Of these replicates one is shown here.

Regarding the distribution of these substances, the humins treated wood seemed to show a more frequent filling of lumina compared to the furfurylated specimens (compare Fig. 2D–F). As the WPG was similar for the two treatments, a smaller percentage of the humins entered the wood cell walls compared to the case of FA used for regular furfurylation. This is as expected, as the humins used for impregnation comprised not only monomers, but also oligomers, which would not as easily penetrate into the dense wood cell walls as FA. Regarding the fluorescence properties of the specimens, Fig. 3 shows that while the untreated wood shows little emission for the excitation wavelengths selected here (Fig. 2A and B as well as Fig. 3A and B), both the furfurylated and the humin treated wood specimens show fluorescence (Fig. 2C, D, E and F as well as Fig. 3C, D, E and F). The emission curves in Fig. 3 also show that the fluorescence from the furfurylated wood agrees with earlier results,[46] *i.e.* emission in the 500–600 nm range for excitation at 488 nm and weak emission in the 650–700 nm range for excitation at 633 nm. The finding that the lignin-rich middle lamellas and cell corners show the most emission is also confirmed (Fig. 3C and D). This is assumed to be caused by the hydrophobic linear conjugated furan chains to predominantly be present in the relatively hydrophobic lignin-rich parts of the wood cell wall. Fig. 3C also confirms that emission is somewhat red-shifted for the PFA polymer in cell lumina compared to the polymer in the wood cell wall, presumably due to longer chains being able to form in the lumina. Regarding the fluorescence properties of the humin treated specimens, the same over-all pattern is seen as for the furfurylated wood, except that fluorescence appears to be somewhat weaker for the cell walls and markedly weaker from the polymer-filled cell lumina (Fig. 2C *vs.* 2E and 2D *vs.* 2F as well as Fig. 3C *vs.* 3E and 3D *vs.* 3F). Provided that the difference in intensity can be linked to the amount of fluorophores present, this would suggest that linear conjugated furan chains are not as abundant in the humin treated specimens as in the furfurylated ones, either because they are simply not formed from the less homogeneous population of molecules in the impregnation liquid used for the humin treatment, or because the polymerisation to a higher extent has reached the later polymerisation step, where Diels–Alder linkages between the linear chains reduce their fluoresence.[47] From the postulated structure of cured humins[43] there is less electronic conjugation compared to PFA which then implies that fluorescence should be weaker for humin-treated wood.

The CLSM results show that the humins penetrated into the cell walls, and that the polymer formed at that location was similar to the polymer resulting from furfurylation using FA.

The scanning electron microscopy (SEM) images in Fig. SI-2† corroborate the CLSM observations. They illustrate that both humins and PFA were well incorporated inside the wood, and that the final internal structure of the two modified samples is very similar. The typical honeycomb structure of wood is well preserved. Both PFA and humins have induced a swelling of the cell wall.

Properties of modified wood

This part aims at highlighting the modification of wood properties after treatment with the two biobased resins. Mechanical, thermal, water and fire properties of humins and PFA modified wood are compared to untreated wood.

First, DMA was used to study the variation of wood mechanical properties after the modification process. Wood treatment might also change the inner structure of wood, thus decreasing the mechanical properties of the samples.[48] Fig. 4 shows the storage modulus and tan δ variation with temperature.

The results highlight an increase in storage modulus after modification with humins for temperatures up to 140 °C, after which the storage modulus of modified wood starts to decrease. The value of storage modulus for humins modified wood is very similar to PFA modified wood for temperatures below 25 °C, and deviate for higher temperatures (>75 °C). The lower storage modulus observed for humin modified wood is explained by considering that a temperature increase affects the mobility of the polymer chains within the wood, which are less rigid in the case of humins compared with PFA. These phenomena can be better identified by observing tan δ variation. The tan δ curve of humin modified wood shows a sharp increase starting from 125 °C, which is observed at 150 °C in PFA modified wood but is not observed in blank wood. This behavior might be due to the cooperative α-relaxation process of humins and PFA, respectively, which can be approximated with their glass transition temperature (T_g). For temperatures below T_g, the tan δ value of humins and PFA modified wood is lower than that of blank wood, indicating a denser and more rigid wood structure. It is worth noting that above 25 °C, the tan δ values of humin modified wood become higher than those of PFA modified wood. Blank wood shows two weak relaxation peaks around 25 °C and 100 °C. The first peak is related to the β-transition of cellulose while the softening at 100 °C is related to the glass transition of lignin.[49] These peaks are less visible after modification with humins or PFA,

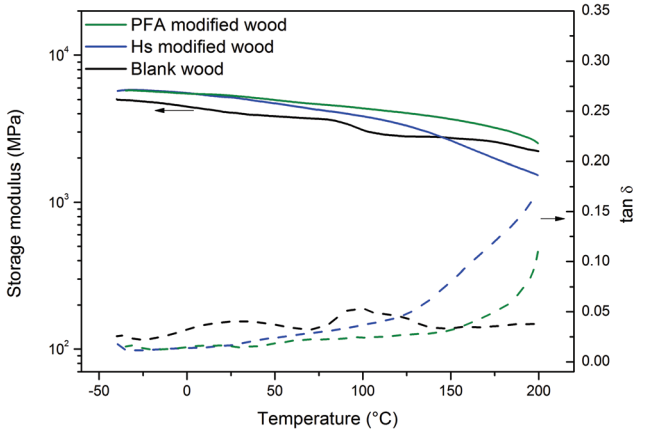

Fig. 4 Storage modulus (solid lines) and tan δ (dashed lines) variation with temperature for blank wood (black lines), humin modified wood (blue lines) and PFA modified wood (green line).

again indicating that the cellulose and lignin environment have been modified.

In summary, the DMA results highlight the similar thermo-mechanical behavior between humin- and PFA-modified wood for temperatures below 75 °C. In the service temperature of wood (*i.e.* between −25 °C to 40 °C) the increase of the elastic modulus for the two modified woods is about 20–25% compared to untreated wood. Such an increase can be connected to the rigidity of the wood board which can be useful for outdoor applications where stiffness is needed. Modified wood can thus compete with traditional hardwood of higher elastic modulus. A higher elastic modulus is also consistent with lower shrinkage in the service temperature.

In addition to the mechanical properties, the thermal behavior of wood is another important property. Therefore, the thermal stability of modified wood was studied by TGA. Fig. 5a shows the TGA scans for blank wood, humin modified wood, PFA modified wood and humin resin with a zoom in the region between 35 °C and 220 °C.

A loss of 7 wt% for blank wood and 3 wt% for humin and PFA modified wood are clearly observed around 100 °C. This step corresponds to the release of weakly bonded water and is linked to the moisture content in the samples. This water content is significantly lower in humin and PFA modified wood and comparable for the two modified samples. This indicates that wood modified with humins obtained a lower equilibrium moisture content (EMC) at 50% of relative humidity and 20 °C, and that its EMC is similar to that obtained by furfurylation for the same WPG (*i.e.* 30%). The wood decay by fungi is directly proportional of the EMC in wood.[7] A significant reduction of the EMC would guarantee higher decay resistance compared to untreated wood especially for bulking modification such as acetylation or furfurylation.[50] Three main degradation steps are observed at a higher temperature in wood samples. The first and second steps occurring between 250 °C and 400 °C, correspond to the degradation of hemicellulose and cellulose, respectively.[51] The maximum rate of weight loss, identified by the peak in DTG (Fig. 5b), occurs around 315 °C for all the samples. The degradation is slower in the case of humin modified wood compared with PFA modified wood and blank wood. The third and last degradation peak, corresponding to the final carbonization of char residue, is observed at 420 °C in humin modified wood and blank wood while it is slightly shifted towards a higher temperature in the case of PFA modified wood. The weight loss between 180 °C and 250 °C is only observed in the modified wood and in the humin sample. This is most probably due to the release of volatile and monomeric furans.[43]

The stability of modified wood after immersion in water was also studied. Fig. 6 shows the thickness increase as function of time after immersion in water for both untreated and modified woods. Humin modified wood reaches saturation after just 1 hour, with a final thickness increasing by 1%, thus showing slightly improved stability in water compared with PFA modified wood, which reaches saturation after 1.5 h with a final thickness increase of 1.6%. Blank wood reaches saturation after 5 hours of immersion in water, with an increase of 5%.

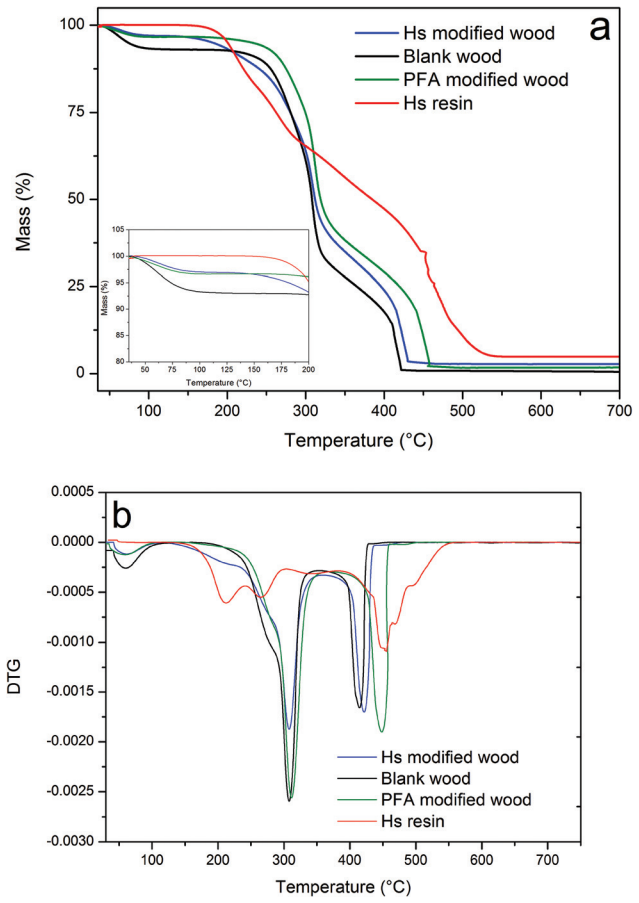

Fig. 5 (a) TGA and (b) DTG measurement under air of blank wood (black line), humin modified wood (blue line), PFA modified wood (green line) and humin resins (red line).

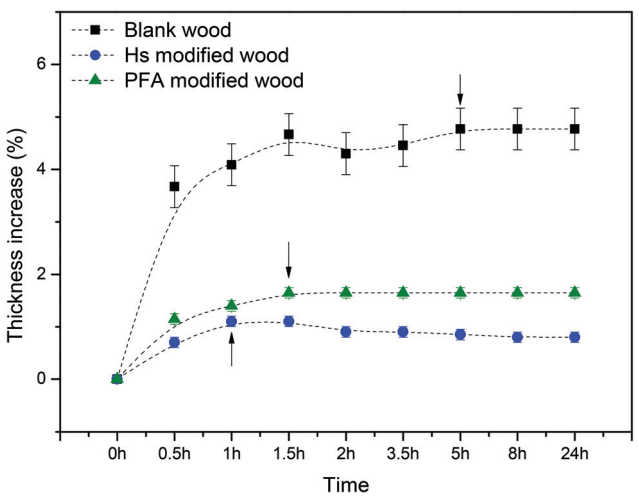

Fig. 6 Thickness increase of blank wood, humin modified wood and PFA modified wood after immersion in water.

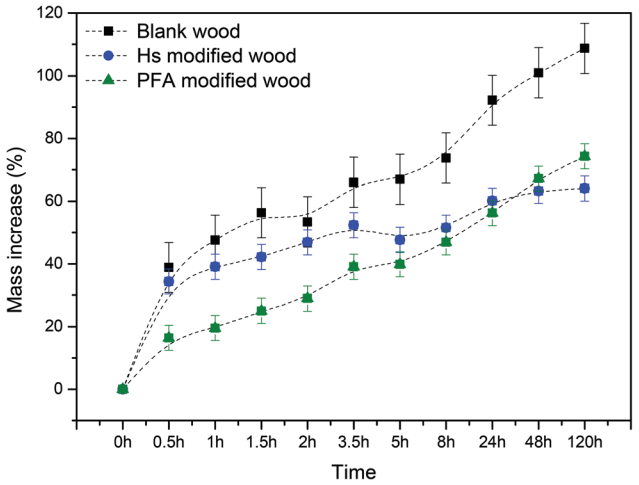

Fig. 7 Mass increase *vs.* time (left axis) for blank wood, humin and PFA modified wood after immersion in water.

Table 3 Burning behavior of blank wood, humin impregnated wood and PFA impregnated wood under well-ventilated fire conditions

Measured parameters	Blank wood	Humin modified wood	PFA modified wood
Sample mass (g)	10.2	13	13.3
Mass loss (%)	100	96.2	97.7
Time for ignition (s)	76	60	54
Average mass loss rate (g m^{-2} s^{-1})	34	43.3	47.5
Max mass loss rate (g m^{-2} s^{-1})	58.2	69.8	184.5
Carbon mass balance (%)	100.5	99.8	101.4
Peak HRR (kW m^{-2})	643	819	945
Residue (g)	0	0.5	0.3
CO/CO_2	0.02	0.02	0.05
Yields of major combustion products			
CO_2 (mg g^{-1})	1527	1573	1549
CO (mg g^{-1})	37.7	35.5	69.9
Soot (mg g^{-1})	13	12.2	18.6
THC (mg g^{-1})	0.8	2.2	7.3
CH_4 (mg g^{-1})	0.1	0.3	1.1

The same test was done to check the increase in mass of the samples (Fig. 7). The three samples show a steep weight increase in the first 0.5 h after immersion in water. As also seen *via* SEM analyses, the voids within the wood lumen were preserved, allowing water to enter into the wood structure. The most interesting differences are observed after long times of immersion in water. After the first hour, the weight increases by around 35%, reaching saturation after 48 hours with an increment in weight of 60% in the case of humin modified wood. PFA modified wood's increase in weight is slower in the first hours but finally shows a larger weight increase (73%, after 120 hours). The weight of blank wood steadily increases without reaching saturation even after 120 hours, increasing the weight up to more than 100%.

These results suggest that the dimensional stability of humin modified wood is significantly improved after the treatment. By bulking the wood cell walls, humins decrease the hygroscopic nature of wood.[52]

The fire risk was assessed for humins and PFA modified wood in comparison with untreated wood. Table 3 gives a summary of the results obtained by testing the materials with the fire propagation apparatus under well-ventilated fire conditions. Fig. 8 shows the peak heat release rate (HRR), and cumulative energy released in the combustion tests of blank wood, humin modified wood and PFA modified wood samples.

Fig. 8 shows that all materials demonstrated some initial resistance to ignition under the test conditions. The combustion tests led to nearly complete combustion of all tested samples. This is reflected by the amount of residue remaining at the end of the combustion process *i.e.* 0 g, 0.5 g and 0.3 g (Table 3), corresponding to 0%, 3.8% and 2.3% of the initial sample mass respectively for blank wood, humin modified wood and PFA modified wood. Humin impregnated wood seems to present some advantages over PFA in terms of resistance to ignition. First, the ignition time is slightly longer (*i.e.*

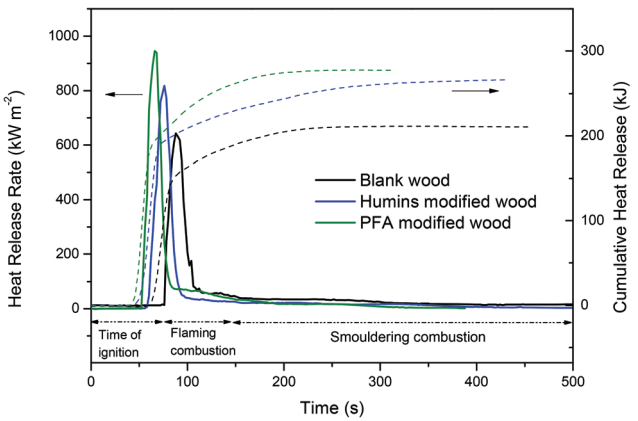

Fig. 8 Heat release rate (solid lines) and cumulative heat release (dashed lines) profiles of blank wood, humin modified wood and PFA modified wood under fire conditions.

60 s instead of 54 s in the case of PFA). Moreover, concerning thermal impact, humins (819 kW m^{-2}) also look like a better option than PFA (945 kW m^{-2}) in terms of peak heat release rates (~13% less in humins than in PFA) for the same amount of wood in the test samples. The cumulative energy release profile from sample combustion *versus* time is also presented in Fig. 8. The overall heat release is only slightly increased in humin modified wood and PFA modified wood samples due to the contribution of the added impregnation media as compared to blank wood.

Finally, the yields of combustion products were assessed and only the carbon-based species such as CO_2, CO, and soot (assumed to be 100% carbon) were measured for the first fire induced toxicity assessment. As reflected by the CO/CO_2 molar ratios (Table 3), all samples were tested under the targeted well-ventilated conditions, which generally prevail in the early stages of fires. Under these oxidative conditions, carbon was

essentially converted into CO_2, together with limited amounts of CO and soot.

Irrespective of the type of impregnation, the experimental CO yields in both humins modified wood and PFA modified wood are very low compared to the maximum theoretical yields (see ESI† for details) which is a classical behavior observed in any cellulosic well-ventilated fire. Thus, the resultant CO yield from PFA tests does not indicate significant concerns from impregnation in terms of CO toxicity under well-ventilated conditions. In addition, we again see a slight advantage in humins as the impregnation medium as compared to PFA in terms of fire induced toxicity. CO yields 69.9 mg g^{-1} of CO in PFA modified wood and it goes down to 35.5 mg g^{-1} of CO for humin modified wood. This statement is also reinforced from the soot yields comparison that similarly brings some advantages to humins.

Conclusion

This work focused on the study of a possible alternative way to modify wood by proposing a novel valorization strategy for humins. A liquid fraction of humins can be extracted from raw biorefinery humins. The low molecular weight and the high functionality of the furanic oligomers contained in the liquid fraction of humins allowed good impregnation in the wood tissues and interaction with wood components as attested by the CLSM results. The resulting humin-modified wood showed enhanced dimensional and water stability after immersion in water, without compromising the mechanical properties, with final properties comparable with PFA modified wood. This solution aims at solving the main issues of wood in outdoor applications by using a resin which is not prepared using toxic chemicals. From the fire safety viewpoint, it was demonstrated that impregnation does not significantly impact the fire hazard of wood. Through the proof of concept of this study, "*humination*" of wood can thus be considered as another type of furfurylation of wood starting from side stream oligomers instead of pure furfuryl alcohol. Moreover, *humination* of wood would also increase the value of humin by-products, with a great impact on the environmental and economic assessment of biorefineries which have to deal with humin formation. In conclusion, *humination* of wood could become a promising alternative for improving wood properties in a green and sustainable way.

Conflicts of interest

There are no conflicts to declare.

Acknowledgements

The authors acknowledge the EU framework Program Horizon 2020 for financial support as in the HUGS project (ID: 675325). The authors would also like to thank Synvina C.V. for providing humin samples and for scientific support. CLSM data were collected at the Center for Advanced Bioimaging (CAB) Denmark, University of Copenhagen.

References

1 J. M. Pin, N. Guigo, A. Mija, L. Vincent, N. Sbirrazzuoli, J. C. Van Der Waal and E. De Jong, Valorization of biorefinery side-stream products: Combination of humins with polyfurfuryl alcohol for composite elaboration, *ACS Sustainable Chem. Eng.*, 2014, **2**, 2182–2190.
2 L. Filiciotto, A. M. Balu, J. C. Van der Waal and R. Luque, Catalytic insights into the production of biomass-derived side products methyl levulinate, furfural and humins, *Catal. Today*, 2018, **302**, 2–15.
3 C. Hill, *Wood modifications: Chemical, Thermal, and other Processes*, Wiley, 2006.
4 C. Risbrudt, *Wood and Society*, 2012.
5 M. Deka and C. N. Saikia, Chemical modification of wood with thermosetting resin: effect on dimensional stability and strength property, *Evaluation*, 2000, **73**, 179–181.
6 F. Kollmann and W. A. Cote, *Principles of wood science and technology*, 1968, vol. d.
7 E. E. Thybring, The decay resistance of modified wood influenced by moisture exclusion and swelling reduction, *Int. Biodeterior. Biodegrad.*, 2013, **82**, 87–95.
8 E. E. Thybring, International Biodeterioration & Biodegradation Water relations in untreated and modified wood under brown-rot and white-rot decay, *Int. Biodeterior. Biodegrad.*, 2017, **118**, 134–142.
9 G. Falco, N. Guigo, L. Vincent and N. Sbirrazzuoli, Opening Furan for Tailoring Properties of Bio-based Poly (Furfuryl Alcohol) Thermoset, *ChemSusChem*, 2018, **11**, 1805–1812.
10 G. Falco, N. Guigo, L. Vincent and N. Sbirrazzuoli, FA polymerization disruption by protic polar solvents, *Polymer*, 2018, **10**, 1–14.
11 M. Westin, Development and evaluation of new alternative wood preservation treatments.pdf, Final Rep. to Swedish Counc. For. Agric. Res.
12 S. Lande, M. Westin and M. Schneider, Properties of furfurylated wood, *Scand. J. For. Res.*, 2004, **19**, 22–30.
13 https://kebony.com/en/content/technology. Consulted December 2019.
14 I. Van Zandvoort, Y. Wang, C. B. Rasrendra, E. R. H. Van Eck, P. C. A. Bruijnincx, H. J. Heeres and B. M. Weckhuysen, Formation, molecular structure, and morphology of humins in biomass conversion: Influence of feedstock and processing conditions, *ChemSusChem*, 2013, **6**, 1745–1758.
15 S. K. R. Patil and C. R. F. Lund, Formation and Growth of Humins via Aldol Addition and condensation during Acid Catalyzed conversion of 5-Hydroxymethylfurfural.pdf, *Energy Fuels*, 2011, 4745–4755.
16 G. Tsilomelekis, M. J. Orella, Z. Lin, Z. Cheng, W. Zheng, V. Nikolakis and D. G. Vlachos, Molecular structure, mor-

phology and growth mechanisms and rates of 5-hydroxymethyl furfural (HMF) derived humins, *Green Chem.*, 2016, **18**, 1983–1993.

17 Z. Cheng, J. Everhart, G. Tsilomelekis, V. Nikolakis, B. Saha and D. Vlachos, Structural Analysis of Humins Formed in the Brønsted-Catalyzed Dehydration of Fructose, *Green Chem.*, 2018, **20**, 997–1006.

18 P. Tosi, G. P. M. van Klink, A. Celzard, V. Fierro, L. Vincent, E. de Jong and A. Mija, Auto-crosslinked rigid foams derived from biorefinery by-products, *ChemSusChem*, 2018, **11**(16), 2797–2809.

19 S. Constant, C. S. Lancefield, B. M. Weckhuysen and P. C. A. Bruijnincx, Quantification and Classification of Carbonyls in Industrial Humins and Lignins by ^{19}F NMR, *ACS Sustainable Chem. Eng.*, 2017, **5**, 965–972.

20 A. Muralidhara, P. Tosi, A. Mija, N. Sbirrazzuoli, C. Len, V. Engelen, E. de Jong and G. Marlair, Insights on thermal and fire hazards of humins in support of their sustainable use in advanced biorefineries, *ACS Sustainable Chem. Eng.*, 2018, **6**(12), 16692–16701.

21 L. Filiciotto, A. M. Balu, A. A. Romero, E. Rodríguez-Castellón, J. C. van der Waal and R. Luque, Benign-by-design preparation of humin-based iron oxide catalytic nanocomposites, *Green Chem.*, 2017, **19**, 4423–4434.

22 S. Lande, M. Eikenes and M. Westin, Chemistry and ecotoxicology of furfurylated wood, *Scand. J. For. Res.*, 2004, **19**, 14–21.

23 S. Lande, M. Eikenes, M. Westin and M. H. Schneider, Furfurylation of wood: Chemistry, properties, and commercialization, *ACS Symp. Ser.*, 2008, **982**, 337–355.

24 P. J. DiNenno, D. Drysdale, C. L. Beyler, W. D. Walton, R. L. P. Custer, J. J. R. Hall and J. M. Watts, *SFPE Handbook of Fire Protection Engineering*, 1995.

25 G. G. Eshetu, S. Jeong, P. Pandard, A. Lecocq, G. Marlair and S. Passerini, Comprehensive Insights into the Thermal Stability, Biodegradability, and Combustion Chemistry of Pyrrolidinium-Based Ionic Liquids, *ChemSusChem*, 2017, **10**, 3146–3159.

26 A. O. Diallo, A. B. Morgan, C. Len and G. Marlair, An innovative experimental approach aiming to understand and quantify the actual fire hazards of ionic liquids, *Energy Environ. Sci.*, 2013, **6**, 699–710.

27 ISO/TR 16312-2:2007 (Ed1) - Guidance for assessing the validity of physical fire models for obtaining fire effluent toxicity data for fire hazard and risk assessment - Part 2: Evaluation of individual physical fire models, ISO, 2007.

28 G. Mantanis, Chemical Modification of Wood by Acetylation or Furfurylation: A Review of the Present Scaled-up Technologies, *BioResources*, 2017, **12**, 4478–4489.

29 https://www.mazzon.eu/en/news/furfuryl-alcohol-price-has-gone-sky-high.

30 https://www.nsenergybusiness.com/pressreleases/companies/future-market-insights/global-furfuryl-alcohol-market-expected-to-reach-us-1493-7-mn-by-2028-driven-by-growth-in-the-foundry-industry-future-market-insights/.

31 Discussion with the Humins' Department of Avantium.

32 A. Sangregorio, N. Guigo, J. C. van der Waal and N. Sbirrazzuoli, All 'green' composites comprising flax fibres and humins' resins, *Compos. Sci. Technol.*, 2019, **171**, 70–77.

33 A. Sangregorio, N. Guigo, J. C. van der Waal and N. Sbirrazzuoli, Humins from biorefinery as thermo-reactive macromolecular systems, *ChemSusChem*, 2018, **11**, 4246–4255.

34 P. T. Anastas and J. C. Warner, Principles of green chemistry, in *Green Chem. Theory Pract.*, 1998, pp. 29–56.

35 A. Muralidhara, A. Bado-Nilles, G. Marlair, V. Engelen, C. Len and P. Pandard, Humins in the environment: early stage insights on ecotoxicological aspects, *Biofuels, Bioprod. Biorefin.*, 2018, 1–7.

36 https://echa.europa.eu/substance-information/-/substanceinfo/100.002.388.

37 J. Franko, L. G. Jackson, A. Hubbs, M. Kashon, B. J. Meade and S. E. Anderson, Evaluation of Furfuryl Alcohol Sensitization Potential Following Dermal and Pulmonary Exposure: Enhancement of Airway Responsiveness, *Toxicol. Sci.*, 2012, **125**, 105–115.

38 C. Hill and A. Norton, The environmental impacts associated with wood modification balanced by the benefits of life extension, *Eur. Conf. Wood Modif.*, 2014.

39 S. T. Barsberg and L. G. Thygesen, *A Combined Theoretical and FT-IR Spectroscopy Study of a Hybrid Poly (furfuryl alcohol) – Lignin Material: Basic Chemistry of a Sustainable Wood Protection Method*, 2017, vol. 2, pp. 10818–10827.

40 B. Mohebby, Application of ATR infrared spectroscopy in wood acetylation, *J. Agric. Sci. Technol.*, 2008, **10**, 253–259.

41 J. S. Rasmussen, S. Barsberg, T. M. Venas and C. Felby, Assessment of covalent bond formation between coupling agents and wood by FTIR spectroscopy and pull strength tests, *Holzforschung*, 2014, **68**, 799–805.

42 C. G. Boeriu, D. Bravo, R. J. A. Gosselink and J. E. G. Van Dam, Characterisation of structure-dependent functional properties of lignin with infrared spectroscopy, *Ind. Crops Prod.*, 2004, **20**, 205–218.

43 A. Sangregorio, N. Guigo, J. C. van der Waal and N. Sbirrazzuoli, Humins from biorefineries as thermo-reactive macromolecular systems, *ChemSusChem*, 2018, **11**, 4246–4255.

44 B. Wladislaw, A. Giora and G. Vicentini, The Syntheses and Infrared Spectra of Some Acetals and Ketals, *J. Chem. Soc. B*, 1966, 586–588.

45 J. S. Lupoi, E. Gjersing and M. F. Davis, Evaluating lignocellulosic biomass, its derivatives, and downstream products with Raman spectroscopy, *Front. Bioeng. Biotechnol.*, 2015, **3**, 1–18.

46 L. G. Thygesen, S. Barsberg and T. M. Venås, The fluorescence characteristics of furfurylated wood studied by fluorescence spectroscopy and confocal laser scanning microscopy, *Wood Sci. Technol.*, 2010, **44**, 51–65.

47 M. Choura, N. M. Belgacem and A. Gandini, Acid-Catalyzed Polycondensation of Furfuryl Alcohol: Mechanisms of Chromophore Formation and Cross-Linking, *Macromolecules*, 1996, **29**, 3839–3850.

48 B. M. Esteves and H. M. Pereira, Wood modification by heat treatment: A review, *BioResources*, 2009, **4**, 370–404.
49 N. Sun, S. Das and C. E. Frazier, Dynamic mechanical analysis of dry wood: Linear viscoelastic response region and effects of minor moisture changes, *Holzforschung*, 2007, **61**, 28–33.
50 R. Ringman, A. Pilgard, C. Brischke and K. Richter, Mode of action of brown rot decay resistance in modified wood: A review, *Holzforschung*, 2014, **68**, 239–246.
51 L. Costes, F. Laoutid, S. Brohez and P. Dubois, Bio-based flame retardants: When nature meets fire protection, *Mater. Sci. Eng., R*, 2017, **117**, 1–25.
52 L. Kong, H. Guan and X. Wang, In Situ Polymerization of Furfuryl Alcohol with Ammonium Dihydrogen Phosphate in Poplar Wood for Improved Dimensional Stability and Flame Retardancy, *ACS Sustainable Chem. Eng.*, 2018, **6**, 3349–3357.